

A NEW METHODOLOGY FOR PRESENTING HYDRODYNAMICS DATA FROM A LARGE RIVER CONFLUENCE

FARHAD BAHMANPOURI ⁽¹⁾, NAZIANO FILIZOLA ⁽²⁾, MARCO IANNIRUBERTO ⁽²⁾ & CARLO GUALTIERI ⁽³⁾

^(1,4)Department of Civil, Construction and Environmental Engineering, University of Napoli Federico II, Napoli, Italy,
farhad.bahmanpour@unina.it, carlo.gualtieri@unina.it

⁽²⁾Universidade Federal do Amazonas, Manaus, AM, Brazil

⁽³⁾Instituto de Geociências - Universidade de Brasília, Campus Universitário Darcy Ribeiro - ICC Centro, 70910-900 Brasília / DF, Brazil
ianniruberto@unb.br

ABSTRACT

Confluences are very complex fluvial networks where the combination of matter (water and sediment) and energy (flow strength) from two different channels take place. The confluence of Rio Negro, with its black waters, and the Rio Solimões, with its suspended white sediments, is one of the biggest confluences on the earth and attracts thousands of tourists every year near by the city of Manaus, Amazonas – Brazil.

This paper presents the application of a new method to analyze the ADCP data which is using an in-house FORTRAN code in combination with the Tecplot and Surfer Softwares. The method was applied to ADCP transects collected on this confluence within the EU-funded Clim-Amazon Project in two different periods of the hydrological cycle: low flow conditions on 30 and 31 October 2014, during the FS-CNS1 campaign, and relatively high flow conditions on 29 and 30 April 2015, during the FS-CNS2 campaign, both of them included 23 transects. These data were first extracted with WinRiver II software to produce ASCII files. The ASCII files were first processed using the code to derive input files containing the three velocity components, the average backscatter as well as the secondary currents from the Rozovskii method. These data were plotted in Tecplot to gain cross-sectional profiles. Furthermore, as past investigations were limited to the analysis of the depth-averaged quantities, the FORTRAN code was used even to extract the values of the velocity components as well as the backscatter along three layers in the channel: near the bed, at mid-depth and near the water surface. The data were then used to prepare Surfer maps, in a plane contour map format, of these quantities. The analysis of the data along these three layers can provide further findings into the complex three-dimensional structure of the flow at the Negro/Solimões confluence.

Keywords: Environmental Hydraulics, confluence, Hydrodynamics, Amazon Basin, ADCP, Data presentation

1 INTRODUCTION

River channel confluences form important morphological elements of every river system, being points at which rapid changes in flow, sediment discharge and hydraulic geometry must be accommodated. River confluences with complex hydrodynamics and typical morphologies are basic nodes and key features of river systems; they are very important for the routing of water, sediments, and pollutants through a river system and are the focus for a range of fluvial processes (Biron and Lane, 2008). In the last four decades a wide body of theoretical, numerical, experimental and field research has emerged on the fluvial dynamics of river confluences. Because of the difficulties associated with the extrapolation of laboratory results to real cases, field investigations are becoming an increasingly popular tool in the study of confluences (Parsons et al., 2007). To date most experimental studies have focused either on laboratory confluences (Best, 1987) or on small natural confluences (Kenworthy and Rhoads, 1995), whereas an extremely limited number of investigations conducted on large river confluences, i.e. channel widths > 100 m (Lane et al., 2008; Konsoer and Rhoads, 2014). Further, to date numerical studies have generally only focused on simulating the flow structure observed in laboratory (Huang et al., 2002) and small natural confluences (Constantinescu et al., 2011). In terms of numerical simulation, Bradbrook et al. (1988) used the three-dimensional form of the Navier-Stokes equations to simulate the flow in a parallel confluence of unequal depth channels and to investigate the effect of different combinations of velocity and depth ratio between the two tributaries. Shakibainia et al. (2010) used SSIIM2.0, a 3-D numerical model, which was validated and applied to investigate secondary currents, velocity distribution, flow separation, and water surface elevation in different conditions of confluence angle, discharge, and width ratios. Zhong-chao et al. (2011) investigated on the confluence of Yangtze River and Jialing River based on the finite element model of two-dimensional depth-averaged surface-water flow which included the hydraulic behavior at the confluence. Schindfesselet al. (2015) compared experimental results with OpenFOAM to investigate three-dimensional complex flow patterns for three different discharge ratios. Martin-vide et al. (2015) studied the confluence of Toltén River and its tributary the Allipén (south of Chile) to quantify total bedload and to understand the balance between tributary and main river and the bedload distribution in space and texture.

There has been an increasing interest in the use of Acoustic Doppler Current Profilers (ADCPs) to characterize the hydraulic conditions near river engineering structures such as dams, fish passes and groins, as part of ecological and hydromorphological assessment. In order to evaluating, analyzing, and displaying ADCP parameters different methods and softwares have been developed. Some methods just for single process regarding moving-vessel deployments have been described and most involve collection of data along transects (Muste et al., 2004a; Dinehart and Burau, 2005a, 2005b; Szupiany et al., 2007, 2009). For example, Le Bot et al. (2011) presented a methodology, called CASCADE, for extracting ADCP data collected in marine environments along vessel transects and outline a routine to derive spatially-averaged velocities along such transects. Dinehart and Burau (2005a, 2005b) presented a method in which multiple transects can be projected and averaged onto a 2D planar grid to allow analysis of the 3D flow field, whereas Rennie and Church (2010) developed a procedure where spatially-distributed ADCP data can be interpolated onto a planar-horizontal 2D grid covering large areas up to entire channel reaches. Müller et al., (2001) developed a tool, LOG_aFlow W, for interpolation of ADCP-derived velocity onto 2D horizontal planes and 3D volumes using hydrodynamic interpolation in space and time. However, this tool is not specifically designed for mapping of cross-section data, which are often used for analysis of morphodynamics and geomorphological flow processes (Dinehart and Burau, 2005a, 2005b; Parsons et al., 2007; Szupiany et al., 2009). Kim et al. (2007) developed AdcpXP, a post-processing software package for ADCP data that includes spatial- and depth-averaging routines. A freely available software tool, called VMS, includes analytical capabilities for quality assurance of moving-vessel, multiple-transect ADCP data, with the general aim of improving processing and visualization of large, reach-scale ADCP data sets for comparison with results of numerical and physical models (Kim et al., 2009). While useful, none of these ADCP data-processing packages computes three-dimensional velocity components, including components used to identify secondary flow, using techniques employed by the geomorphological process community. Parson et al. (2012) developed a software, called VMT (Velocity Mapping Toolbox), which allows rapid processing (vector rotation, projection, averaging and smoothing), visualization (planform and cross-section vector and contouring), and analysis of a range of ADCP-derived dataset. The output formats for different parameters vorticity, shear velocity, bed shear stress, the longitudinal dispersion coefficient, and suspended sediment concentrations (with a sediment calibration option for acoustic backscatter) in 2D and 3D and in vertical and plan views could be possible. In this study, a new methodology for analyzing and presenting the ADCP data has been introduced.

The paper is structured as it follows: in Section 2 a detailed description of the field site and instrumentation is presented, including the geographic description of the confluence, hydrodynamic properties, devices, measured parameters, etc. Section 3 focuses on the data analyzing and post processing: it first describes the averaging data and extracting graphs, then presenting near surface, mid-depth and near bed data and finally calculation and presentation of secondary velocity.

2 FIELD SITE AND INSTRUMENTATION

The confluence of the Negro and Solimões rivers is located near Manaus in Northern Brazil, where these rivers merge to form the Amazon River approximately 1600 km upstream from its mouth at the Atlantic Ocean. This confluence is famous for the meeting of the black and white waters of the two rivers which is shown in figure 1. As part of the CLIM-Amazon Project, which was a joint European and Brazilian Research Project funded by the EU about climate and sedimentary processes of the Amazon River Basin, two field studies were conducted about that confluence in both low (October 2014, FS-CNS1 campaign) and relatively high flow conditions (April/May 2015, FS-CNS2 campaign) (Trevethan et al., 2015a; 2015b; 2016). In these field trips, acoustic Doppler velocity profiling (ADCP) and high-resolution seismic methods, such as echo-sounding and sub-bottom profiling, were used as well as water sampling for the measurement of several water chemistry parameters (temperature, conductivity, pH, turbidity, dissolved oxygen, oxygen isotopes) and suspended sediments concentration. These data were collected to investigate key features about hydrodynamics, mixing, sediment transport and morphodynamics about this confluence. During both FS-CNS1 and FS-CNS2, a Teledyne RDI 600 kHz Rio Grande acoustic Doppler current profiler (ADCP) was used to collect cross-sectional measurements at key locations about the confluence, as indicated by lines in Figure 2.

During FS-CNS1 water samples at surface, 10 m, and 20 m depths at twelve locations about confluence were collected. These water samples were used to understand the characteristics of the two tributary rivers (temperature, pH, conductivity) and measure local suspended sediment concentration (SST) and oxygen isotope values. In FS-CNS2 vertical physico-chemistry profiles were collected with a YSI EVO2 multi-parameter probe. The locations are indicated by black point in Figure 2 (right). For each vertical profile, this probe collected the variation in temperature, pH, conductivity, turbidity, chlorophyll and dissolved oxygen concentrations with depth. Further water samples were collected at Sites S0 and N0 to measure the local SST concentration on the Solimões and Negro Rivers respectively.

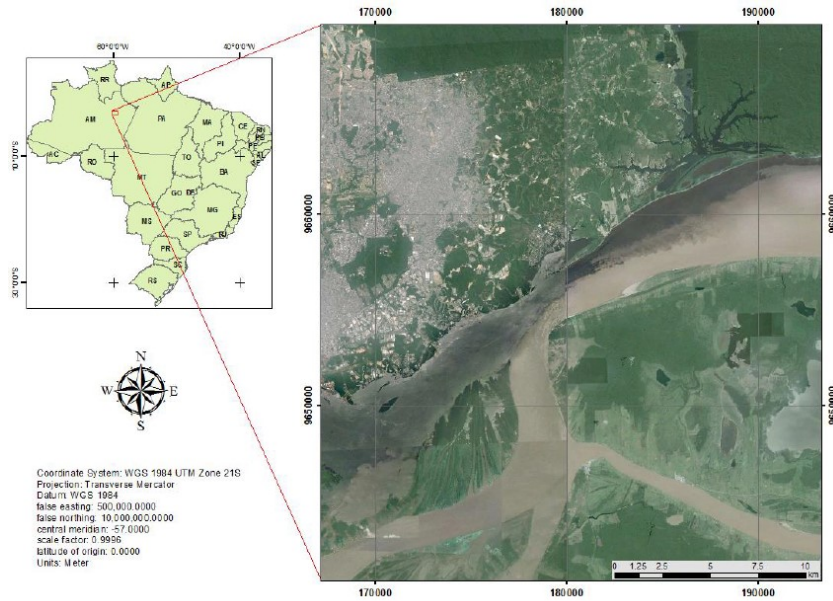


Figure 1. Confluence of the Negro and Solimões rivers near Manaus

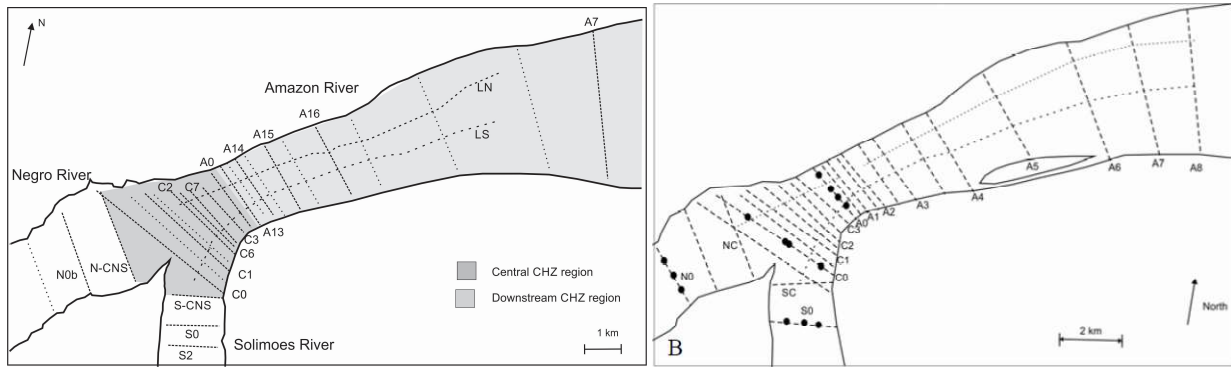


Figure 2. Map of confluence of Negro and Solimões rivers, with sampling positions during Field Study FS–CNS1 (left) and FS–CNS2 (right) are highlighted. Dots show the locations where vertical profiles were collected in FS–CNS2 (Trevethan et al., 2015a; 2016)

Table 1 lists the measured median main flow properties of Negro and Solimões rivers at the ADCP transects just upstream of the confluence (N-CNS and S-CNS, three for each river and each field study) on both the field trips. In Table 1, it can be seen that large differences in discharge and flow velocities are observed in the Solimões River between field studies FS–CNS1 and FS–CNS2, whereas on the Negro River these differences are smaller.

Table 1 – Main flow properties of Negro and Solimões Rivers during FS–CNS1/FS–CNS2

	Field trip	Q (m ³ s)	A (m ²)	W (m)	h _{med} (m)	W/h _{rect} (-)	V _{avg} (m/s)	V _{depth-avg} (m/s)	Dir (°)	V _{max} (m/s)
Negro	FS–CNS1	24510	64784	2830	24.4	117	0.38	0.39	59	0.69
	FS–CNS2	33501	86952	2875	31.2	95	0.38	0.40	58	0.67
Solimões	FS–CNS1	63380	42789	1589	27.2	59	1.49	1.33	289	2.20
	FS–CNS2	105205	61895	1925	28.6	60	1.70	1.52	255	2.59

Legend: Q = discharge; A = cross-sectional area; W = width; h_{med} = median depth; W/h_{rect} = median of the aspect ratio; V_{avg} = median of the cross-section velocity (Q/A); V_{depth-avg} = median of the depth-averaged velocity; Dir = median of flow direction degrees from North; V_{max} = maximum depth-averaged velocity

Previous confluence studies have largely acknowledged that the momentum flux ($M_R = \rho_N Q_N V_{ave-N} / \rho_S Q_S V_{ave-S}$), discharge ($Q_R = Q_N / Q_S$) and velocity ($V_R = V_{ave-N} / V_{ave-S}$) ratios can be related to the observed hydrodynamic and morphodynamic features about the confluence, where the subscripts N and S represent the Negro and Solimões rivers, respectively. These ratios for field studies FS–CNS1 and FS–CNS2 are listed in Table 2.

Table 2. Discharge, velocity and momentum flux ratios FS–CNS1/FS–CNS2

Field trip	Q_R	V_R	M_R
FS–CNS1	0.39	0.25	0.10
FS–CNS2	0.32	0.22	0.07

The relatively high values of these ratios are indicative of the large difference in the flow properties of the two tributary rivers. As discussed in previous studies, high tributary over main river discharge ratio narrows the scour hole and pushes it toward the main river bed, hampering the entry of much of the bedload (Best, 1988; Rhoads et al., 2009).

3 DATA ANALYSIS AND POST-PROCESSING

In order to evaluate the data which had been collected with ADCP; in the first step, the initial raw data were extracted with WinRiver II. The output file of WinRiver II which was in text format contains a large volume of data including different parameters per ensemble with different depth. Since these data were completely unorganized, it required to convert the data to organized format and also an important issue was that the average of all parameters per ensemble required for analyzing the data. In the second step, data were averaged per ensemble with FORTRAN code, and also primary and secondary velocities were calculated. then in the third step, The Surfer13 software was used for plotting graphs based on geographical coordinates for the different type of parameters. Surfer is a full-function contouring and surface modeling package that runs under Microsoft Windows. Surfer is used extensively for terrain modeling, bathymetric modeling, landscape visualization, surface analysis, contour mapping, watershed and 3D surface mapping, gridding, view shed analysis, volumetric, and much more. In order to get an acceptable presentation of graphs for each parameter, based on the statistical criteria, a lot of tries were made for kriging the data especially radius and angle of searching points. In some areas because of transect's location, near or far distance, and river angle with longitudinal coordinate the total area were divided into three or four parts with different kriging setting. And finally, in fourth step secondary velocity with other parameters were plotted using Tecplot. Figure 3 depicts the flowchart of this process.

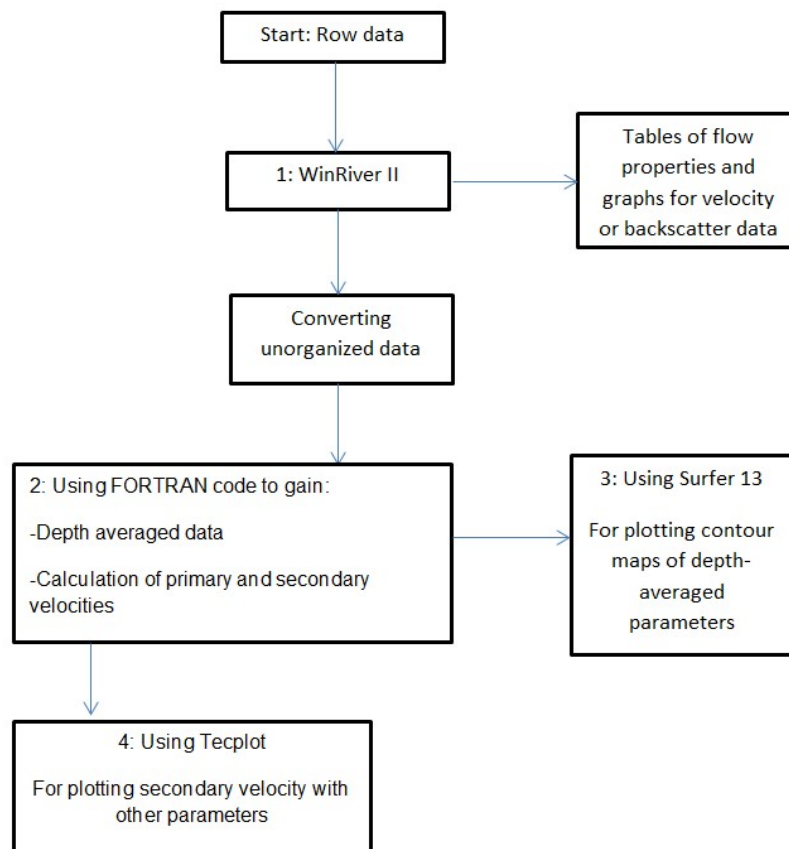


Figure 3. Flow-chart of post-processing of the ADCP data

To compute depth-average velocities, the average value was computed by

$$V_{av} = \frac{1}{d_2 - d_1} \int_{d_1}^{d_2} v dz \quad [1]$$

Where, V_{av} is the depth-averaged velocity and v is the velocity magnitude, north or east component of velocity and d_1 and d_2 are the lower and upper limits of the depth range used in averaging, respectively. for all other parameters this method is used for averaging the data.

Figures 4 and 5 show the depth-averaged velocity and bathymetry for two different days, 30/10/2014 (left) and on 29/04/2015 (right), in relatively low and relatively high flow conditions respectively. The graphs were extracted with Surfer 13 software. Maps of the channel bed topography (Figure 5) show that at the beginning of the confluence zone although the incoming channels are of a similar depth with no distinct discordance in bed level, for low flow conditions a deep scour is present within the confluence zone at downstream side and for high flow condition it happens in two areas; at Negro side and middle of confluence.

The contours in Figure 4 reveal that how the tributary affected the main flow regime because of the difference of velocities and angle of confluence. It also shows that firstly the maximum velocity region is in the mixing interface and secondly the maximum velocity area for low flow conditions happens at the downside of the Intersection but for relatively high flow conditions, it happens exactly at intersection area. Based on bathymetry the area of maximum scouring, which equal to maximum depth, is exactly at the downside of the area of maximum velocity for low flow conditions but for relatively high flow conditions, the area of maximum velocity exactly coincides with maximum scouring area.

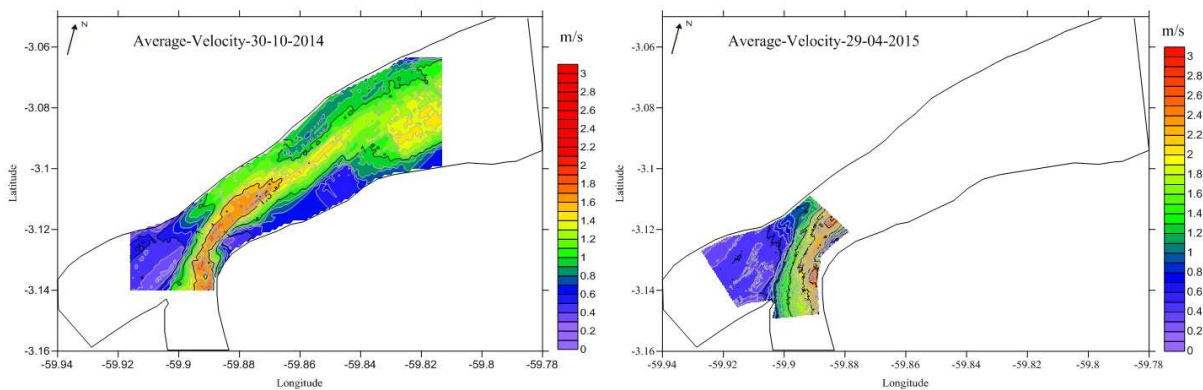


Figure 4. Depth-averaged velocity for low flow conditions (left) and relatively high flow conditions (right)

Based on Best model (1987) for key hydrodynamic features about a confluence, all morphological features could be seen about this confluence include: separation zone, flow deflection zone, separation zones, maximum velocity and a scour hole normally orientated along the region of maximum velocity where both flows begin to converge and finally flow recovery.

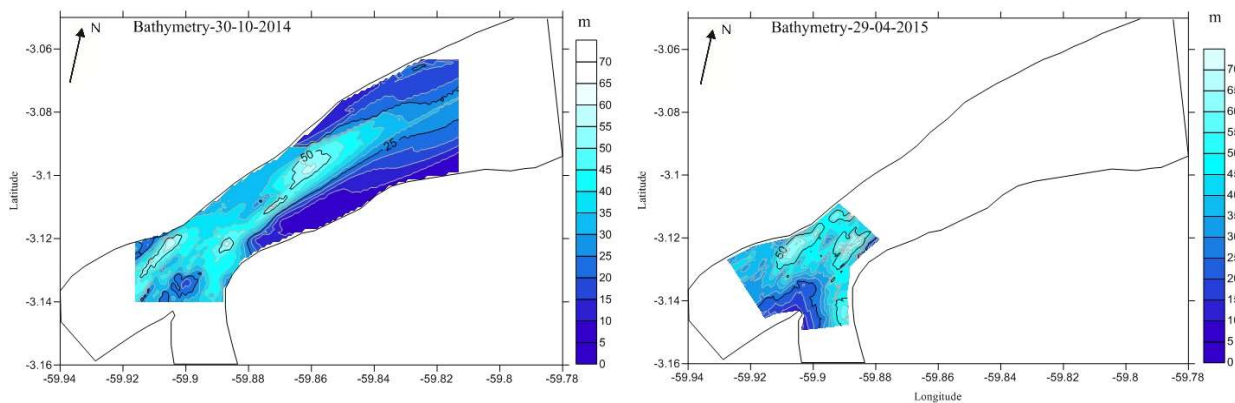


Figure 5. Bathymetry for low flow conditions (left) and relatively high flow conditions (right)

Figure 6 presents the velocity contours in three different layers; near surface, mid-depth and near-bed for two days in low and relatively high flow conditions. Velocity near surface is higher than mid-depth and near bed areas and in both days, maximum velocity for upper and lower layers, near surface and near bed, are higher

than velocity in mid-depth layer. There are three possible reasons for this phenomenon: first the effect of river bend, second the effect of variation in bed topography and third the effect of difference in rivers flow density.

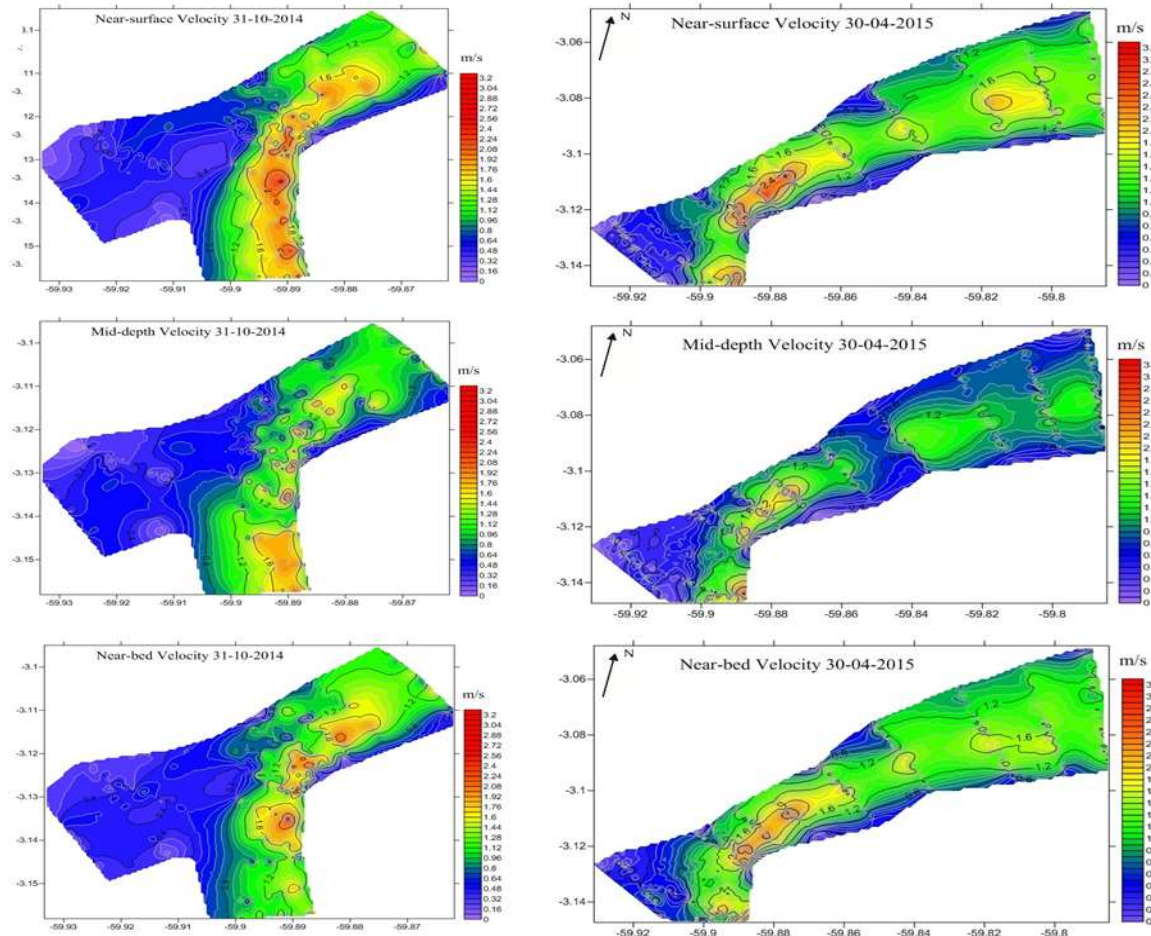


Figure 6. Velocity in three different regimes for low flow conditions (right) and relatively high flow conditions (left)

Since in the confluence zone the effect of river bend and difference in density is low, here the focus is on the bed level discrepancy. As previous studies, (Trevethan et al. (2015)) have been investigated on the topography of this confluence there is large hole, length 1500m, width 700m, depth 20m in the middle part and a small hole like V-shaped valley, width 150m, height 5m, in Negro side of cross section. Therefore these variation in bed topography could result in changing velocity profile and as Parson et al. (2007) based on studies on a large confluence in Rio Paraná Argentina stated, the discordance in bed height between the combining flows is known to produce a zone of negative dynamic pressure in the lee of the shallower channel, resulting in downstream advection and upwelling of fluid from the deeper channel into the waters of the shallower channel. Shugar et al. (2010) based on investigation on the Rio Paraná Argentina asserted that coherent flow structure is generated by dunes which result in the cyclic pattern of upwelling and down welling fluid over the dune crest. In other words, Phase coherence wavelet analysis shows that streamwise and vertical velocities are strongly and inversely correlated over the dune crest, where flow decelerations are linked to fluid upwelling and vice versa. Rhoads and Kenworthy (1995) elucidated two main features of helical motions: (1) the direction of the primary velocity vectors changes consistently, with maximum deviation angles near the water surface and near the bed and (2) this pattern is maintained across many verticals. Finally, all variations in velocity profiles may be also some evidence of flow acceleration into the confluence and deceleration downstream of the confluence, as reported by Roy et al. (1988) and Roy and Bergeron (1990).

One approach to exploring the existence of helical motion at confluences is to decompose the cross-stream velocity at each point in a vertical into components oriented parallel and orthogonal to the depth-averaged velocity vector at this vertical (Rhoads and Sukhodolov, 2001). Primary and secondary velocities were calculated based on Rozovskii method as used by Lane et al (2000). This method essentially identifies the primary velocity direction for each profile as the depth-integrated flow vector, and the secondary currents are then obtained by the differences from this average vector within the profile. This procedure effectively identifies individual secondary planes at each vertical profile across a given section, thus permitting identification of variations in the primary flow direction within a section, without distorting the secondary flow results (Szupiany et al.

2009). Application of the Rozovskii method followed Rhoads and Kenworthy (1998). Primary (v_p) and secondary components (v_s) of each point velocity in each vertical, as shown in Figure 7, were determined from.

$$v_p = (v_x^2 + v_y^2)^{0.5} \cos(\theta - \phi) \quad [2]$$

$$v_s = (v_x^2 + v_y^2)^{0.5} \sin(\theta - \phi) \quad [3]$$

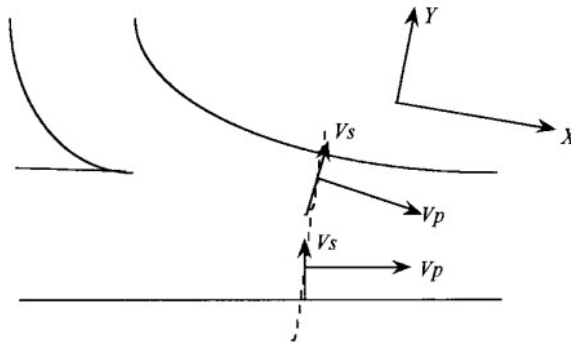


Figure 7. Definition of Rozovskii method (Lane et al. 2000)

Where θ is the orientation of the point velocity vector and ϕ is the orientation of the depth-averaged velocity vector, defined as zero when parallel to x, and becoming positive in an anti-clockwise direction from x. Following both Bathurst et al. (1977) and Rhoads and Kenworthy (1998), ϕ was determined from the direction of the depth-averaged velocity vector defined by integrating v_x and v_y separately over the flow depth for each vertical.

To illustrate the secondary velocity one of transects in the confluence zone for low flow condition, transect CNS6 as shown in figure 2, was used. Figure 8 reveals the calculated secondary flow vectors superimposed on the depth-averaged backscatter contours for two cases, without and with smoothing. Two methods of smoothing were used, first smoothing in Fortran code and second smoothing with Tecplot. For both of graphs smoothing with the code was done, but one without Tecplot smoothing and the other with Tecplot smoothing. Smoothing in the code was done based on averaging three points per ensemble i.e. three points in the vertical direction.

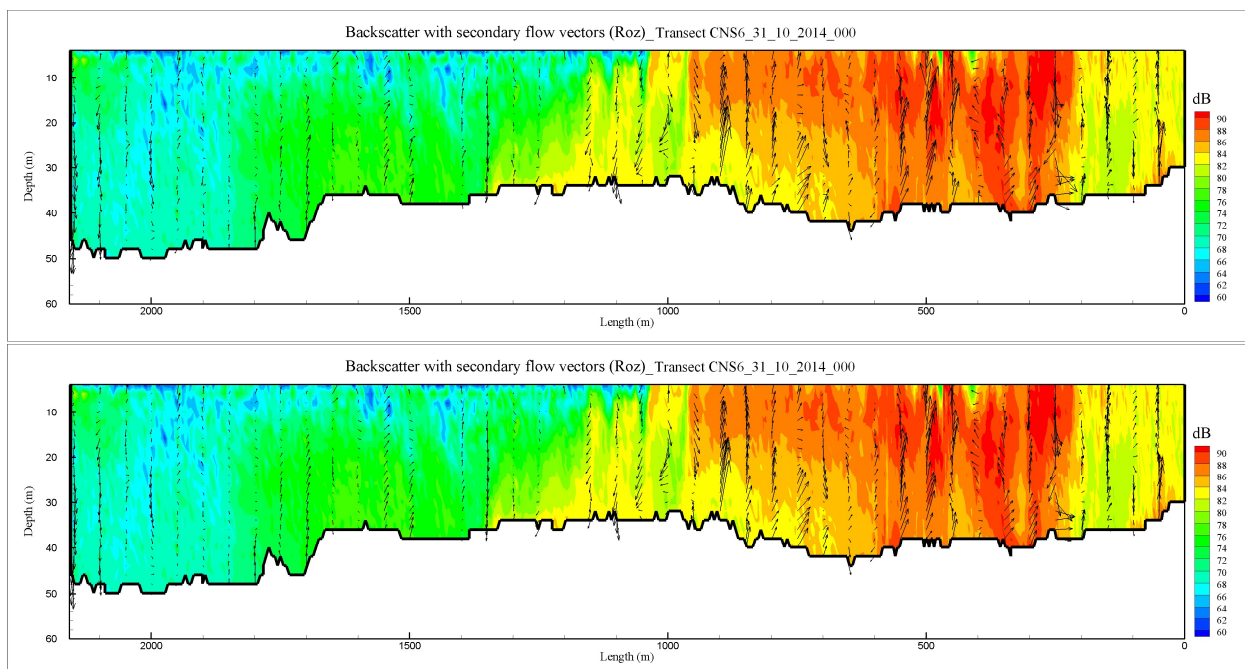


Figure 8. Backscatter with secondary velocity based on Rozovskii method, without smoothing (up) and with smoothing (down). Transect CNS6 on 31/10/2014

For all figures of secondary velocity, sections are viewed looking downstream with the left bank on the left-hand side. Backscatter intensity on the right side of the cross-section is higher than the left side with maximum

90 dB and 82 dB in the right and left sides respectively. The interface line of confluence sharply divide the backscatter range for two rivers and this phenomenon reveals that the mixing process is quite complex.

In Figure 8 right side is in the mouth of Solimões River. Scattered and irregular secondary flow circulation are seen especially in right side of the cross-section. The first or main reason is the high turbulence in the mixing interface of confluence because of the angle of the tributary and the second reason is the difference in momentum flux. Rio Solimões meets the Rio Negro with the angle of 80 degree, therefore it results in creating intense circulation in flow and secondary flow. Changes in bed topography have even an effect. As it can be seen in figure 5 right, the scour hole is in the mixing area which has an important effect on the circulation.

Figure 9 shows the VMT output for the average backscatter data and secondary velocity based on Rozovskii method. The first point is that VMT interpolates available ensemble data with random distance on the length of transect line to the ensembles with fixed distant. So, it results in differences between our code output and VMT output. And the second point is that in order to calculate the secondary velocity, the resultant vector is based on vertical velocity and the velocity in direction y, so that the vertical velocity should be same as original input vertical velocity. But, in VMT the vertical velocity has been changed in the process of calculations. In the FORTRAN code, there is no interpolation and secondary velocity is calculated exactly on the initial location of the ensembles.

Figure 10 illustrates the primary velocity with secondary velocity based on Rozovskii method with smoothing. As it is obvious in the right side the primary velocity is higher. Therefore it again shows that difference in discharge or velocity is the reason that in right side the secondary velocity is stronger and it makes the flow more turbulent. In some areas, vertical velocity is stronger than transverse velocity which results in downward or upward of flow circulation and in some areas, transverse velocity is stronger and results in horizontal flow circulation. Generally, direction of secondary velocity is depends on collision of two rivers, bed topography, primary velocity and channel width.

Depth-averaged primary and secondary velocities based on Rozovskii method are shown in figure 11. The primary velocity is start increasing from middle part toward right bank due to higher discharge rate in Solimões side. Since, depth-averaged secondary velocity is summation of positive and negative velocity values per different layers; So, the average values is restricted between -0.5 to 0.5. The average secondary velocity in Solimões side is greater than on the Negro side.

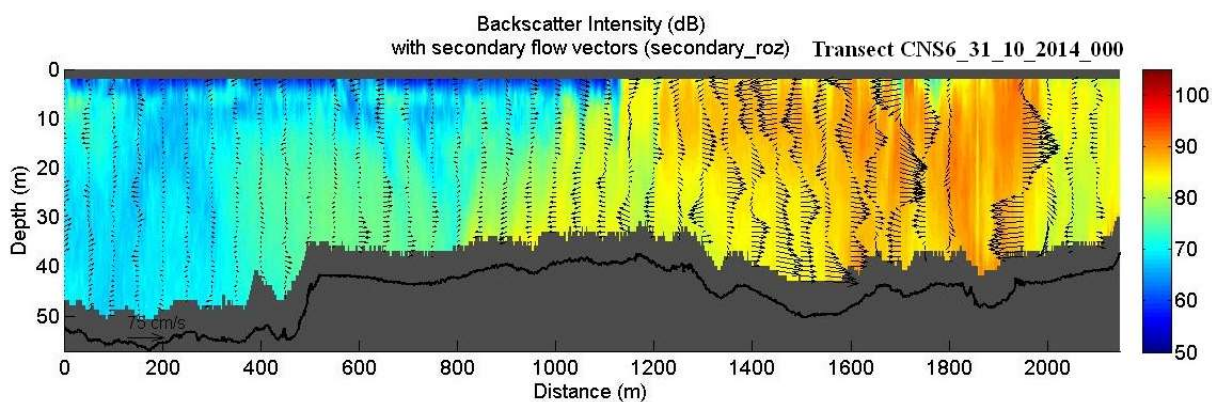


Figure 9. Backscatter with secondary velocity based on Rozovskii method, VMT output. Transect CNS6 on 31/10/2014

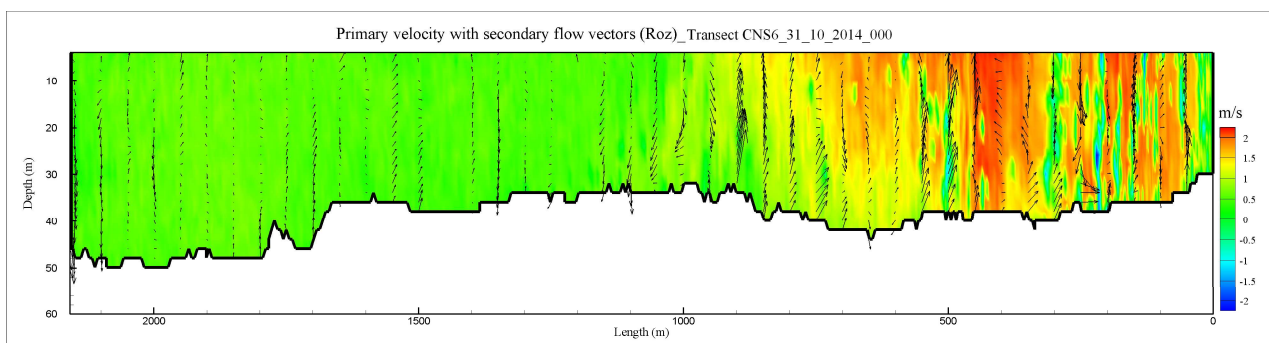


Figure 10. Primary velocity with secondary velocity based on Rozovskii method with smoothing. Transect CNS6 on 31/10/2014

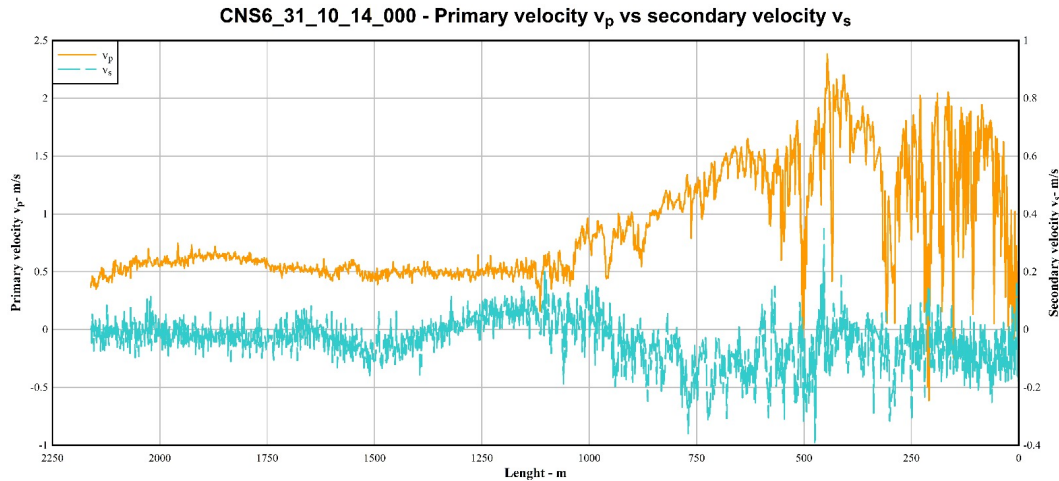


Figure 11. Depth-averaged primary and secondary velocities based on Rozovskii method for transect CNS6 on 31/10/2014

4 CONCLUSIONS

This paper presented a method to analyze and present the ADCP data collected in a large field studies at the confluence of the Negro and Solimões rivers, in Brazil. To illustrate this method, flow properties in this confluence were evaluated. Depth averaged data for different parameters using Surfer software were represented. Second, the complex three-dimensional features of the flow at the confluence requires the analysis of velocity at different depths. Hence, data at the water surface, at mid-depth and near the bed were extracted using Fortran code and then plotted with the Surfer software. Finally, secondary velocities based on Rozovskii method were calculated. The analysis of these velocities showed a complex circulation at the Rio Negro and Rio Solimões. The presented method could be applied to a wide range of applications where flow measurements are conducted along transects using ADCPs.

ACKNOWLEDGEMENTS

The paper is a part of research for PhD degree in Civil System Engineering (31st cycle), at the University of Federico II Napoli, Italy. The authors acknowledge this research was carried out within the Clim-Amazon European Laboratory in Brazil funded by grant agreement FP7 INCO-LAB n° 295091 from the European Commission and the partial support from the MIUR PRIN 2010-2011 Research Project HYDROCAR (CUP n. E61J12000210001). The authors also acknowledge Dr. Mark Trevethan for his collaboration on preparing data and some maps.

References

- Best, J. (1987). Flow dynamics at river channel confluences: implications for sediment transport and bed morphology. *12 Recent Developments in Fluvial Sedimentology*, (Eds. Ethridge, F., Flores, M. and Harvey, M.), Spec. Publ. 39, Society of Economic Paleontologists and Mineralogists, 27-35.
- Best, J. (1988). Sediment transport and bed morphology at river channel confluences. *Geomorphology* 35(3), 481-498.
- Biron, P., and Lane, S. (2008). Modelling hydraulics and sediment transport at river confluences. *River confluences, tributaries and the fluvial network*, (Eds: Rice, S., Roy, A. and Rhoads, B.), J. Wiley & Sons, 17-43.
- Bradbrook, K. F., Biron, P. M., Lane, S. N., Richards, K. S. and Roy, A. G. (1998). Investigation of controls on secondary circulation in a simple confluence geometry using a three-dimensional numerical model. *Hydrol. Process*, 12: 1371-1396.
- Constantinescu, G., Miyawaki, S., Rhoads, B., Sukhodolov, A., and Kirkil, G. (2011). Structure of turbulent flow at a river confluence with a momentum and velocity ratios close to 1: insight from an eddy-resolving numerical simulation. *Water Resources Research*, 47, W05507, 16 pages.
- Dinehart, R. L. and Burau, J. R. (2005a). Repeated surveys by acoustic Doppler current profiler for flow and sediment dynamics in a tidal river. *Journal of Hydrology*. 314:1-21.
- Dinehart, R. L. and Burau, J. R. (2005b). Averaged indicators of secondary flow in repeated acoustic Doppler current profiler crossings of bends. *Water Resources Research*, 41, W09405.
- Kenworthy, S. and Rhoads, B. (1995). Hydrologic control of spatial patterns of suspended sediment concentration at a stream confluence. *Journal of Hydrology*, 168, 251-263.
- Konsoer, K., and Rhoads, B. (2014). Spatial-temporal structure of mixing interface turbulence at two large river confluences. *Environmental Fluid Mechanics*, 14(5), 1043-1070.
- Huang, J., Weber, L. and Lai, Y. (2002). Three-dimensional numerical study of flows in open-channel junctions. *Journal of Hydraulic Engineering*, 128(3), 268-280.

- Kim, D., Muste, M., Mueller, D.S. and Winkler, M. (2009). A quick tutorial for using VMS. *U.S. Army Corps of Engineers*, 68pp. (Online publication accessed October 15, 2012; http://chl.erdc.usace.army.mil/Media/1/1/2/0/VMS_quick_tutorial.pdf).
- Lane, S., Parsons, D., Best, J., Orfeo, O., Kostaschuk, R. and Hardy, R. (2008). Causes of rapid mixing at a junction of two large rivers: Rio Parana and Rio Paraguay, Argentina. *Journal of Geophysical Research*, 113, F02019, 16 pages.
- Le Bot, P., Kermabon, C., Lherminier, P. and Gaillard, F. (2011). CASCADE V6.1: Logiciel de validation et de visualisation des mesures ADCP de coque. Rapport technique OPS/LPO 11–01. Ifremer, Centre de Brest, France; 93.
- Martín-Vide, J.P., Plana-Casado, A., Sambola, A. and Capapé, S. (2015). Bedload transport in a river confluence. *Geomorphology* Volume 250, 1 December 2015, Pages 15-28.
- Muste, M., Yu, K. and Spasojevic, M. (2004a). Practical aspects of ADCP data use for quantification of mean river flow characteristics: Part I: Moving-vessel measurements. *Flow Measurement and Instrumentation* 15:1–16.
- Müller, V., Eden, H. and Vorrath, D. (2001). Flow The Hydraulic Software for Hydraulic Engineering and Navigation. *In Proceedings of the International Conference on Port and Maritime R&D and Technology*, 29–31.10.2001, Shankar NJ, Cheong TA, Pengzhi L (eds). National University of Singapore: Singapore; 953–957.
- Parsons, D., Best, J., Lane, S., Orfeo, O., Hardy, R. and Kostaschuk, R. (2007). Form roughness and the absence of secondary flow in a large confluence-diffuence, Rio Parana, Argentina. *Earth Surface Processes and Landforms*, 32, 155-162.
- Parsons, D., Jackson, P., Czuba, J., Engel, F., Rhoads, B., Oberg, K., Best, J., Mueller, D., Johnson, K. and Riley, J. (2013). Velocity Mapping Tool (VMT): a processing and visualization suite for moving-vessel ADCP measurements. *Earth Surface Processes and Landforms*, 38, 1244-1260
- Rennie, C. D. and Church, M. A. (2010). Mapping spatial distributions and uncertainty of water and sediment flux in a large gravel bed river reach using an acoustic Doppler current profiler. *Journal of Geophysical Research* 115: F03035.
- Rhoads, B.L., and Sukhodolov, A.N. (2001). Field investigation of three-dimensional flow structure at stream confluences: 1. Thermal mixing and time-averaged velocities. *Water Resources Research*, 37(9), 2393–2410
- Rhoads, B.L., Riley, J. D. and Mayer, D.R. (2009). Response of bed morphology and bed material texture to hydrological conditions at an asymmetrical stream confluence. *Geomorphology*, 109(3-4), 161-173.
- Roy, A.G. and Bergeron, N. (1990). Flow and particle paths at a natural river confluence with coarse bed material. *Geomorphology*, 3, 99- 1122.
- Roy, A.G., Roy, R. and Bergeron, N. (1988). Hydraulic geometry and changes in flow velocity at a river confluence with coarse bed material. *Earth Surface Processes and Landforms*, 13, 583-598.
- Schindfessel, L., Créelle, S. and De Mulder, T. (2015). Flow Patterns in an Open Channel Confluence with Increasingly Dominant Tributary Inflow. *Water*, 7, 4724-4751.
- Shakibainia, A., Majdzadeh Tabatabai, M.R. and Zarrati, A.R. (2010). Three-dimensional numerical study of flow structure in channel confluences. *Canadian Journal of Civil Engineering*, 2010, 37 (5), 772-781.
- Shugar, D.H., Kostaschuk, R., Best, J.L., Parsons, D.R., Lane, S. N., Orfeo, O. and Hardy, R.J. (2010) On the relationship between flow and suspended sediment transport over the crest of a sand dune, Río Paraná, Argentina. *Sedimentology*, 57: 252–272.
- Szupiany, R.N., Amsler, M.L., Best, J.L. and Parsons, D.R. (2007). Comparison of fixed- and moving vessel measurements with an aDp in a large river. *J. Hydraul. Eng.*, 133(12), 1299–1310.
- Szupiany, R. N., Amsler, M. L., Parsons, D. R. and Best, J. L. (2009). Morphology, flow structure, and suspended bed sediment transport at two large braid-bar confluences. *Water Resour. Res.*, 45, W05415.
- Trevethan, M., Martinelli, A., Oliveira, M. Ianniruberto, M. and Gualtieri, C. (2015a). Fluid dynamics, sediment transport and mixing about the confluence of Negro and Solimões rivers, Manaus, Brazil. *In 36th IAHR World Congress, The Hague, The Netherlands*, June 28-July 3, 2015, Paper 80094.
- Trevethan, M., Ventura Santos, R., Ianniruberto, M., Santos, A., De Oliveira, M., and Gualtieri, C. (2016). Influence of tributary water chemistry on hydrodynamics and fish biogeography about the confluence of Negro and Solimões rivers, Brazil. *11th International Symposium on EcoHydraulics (ISE 2016)*, Melbourne, Australia, February 2/7, 2016, Paper 25674.
- Zhong-Chao, Y. and Ze-Yi, Y. (2011). Numerical simulation study on hydraulic behaviour at the confluence of Yangtze River and Jialing River. *Procedia Engineering*, Volume 12, 2011, Pages 197-203, 2011, Conference on Engineering Modelling and Simulation (CEMS 2011)